Submitted to
Nuclear Instruments and Methods



UCRL-18969
Preprint



# FIELD CORRECTION WINDINGS FOR IRON MAGNETS

Klaus Halbach

November 1970

AEC Contract No. W-7405-eng-48




UCRL-18969

## DISCLAIMER

# FIELD CORRECTION WINDINGS FOR IRON MAGNETS†

Klaus Halbach

Lawrence Radiation Laboratory
University of California
Berkeley, California 94720

November 1970

Abstract: A method is described that allows modification of the field distribution in the iron-free region of magnets. The field modification is obtained by energizing conductors that are imbedded in the iron. The effects of these correction windings are described and rules are given for their proper placement and excitation.

†This work performed under the auspices of the U. S. Atomic Energy Commission.

## 1. Introduction

One of the difficult problems in the design of iron magnets is to obtain the desired field distribution over a wide range of field levels. A number of methods have been used to counteract the field degradation caused by saturation effects, for instance crenellations[1]) or poleface shaping to obtain good fields simultaneously at low and high field levels[2]). Although these methods give satisfactory results under some circumstances, the achievable field quality is limited. Even more important is the fact that modifications are virtually impossible after the magnet has been built. As the requirements for the field quality of magnets get tighter (homogeneities of the order $10^{-5}$ are now considered for high resolution spectrometers), it seems imperative to be able to control the field distribution after magnet fabrication, and in some instances also during operation. The two main reasons are: a) it seems very difficult to design magnets that achieve such field accuracies over large volumes without the use of free parameters, and even if this could be done on paper, it would be doubtful whether the actual magnet would perform to specifications because of fabrication tolerances, uncertainties about the magnetic properties of the iron, and other imponderables. b) Designing free parameters into the magnet has of course the additional advantage that it allows modification of the field distribution within some limits during operation, if beam optical considerations should require it.

Poleface windings[3]) make it possible to control the field distribution, but their use is often prohibited because of some of the following disadvantages: a) Poleface windings take space and therefore require an increase of the magnet gap. b) The field is severely perturbed in the vicinity of the

poleface windings. This can only be prevented by another substantial increase of the gap, or by having a nearly continuous distribution of poleface windings, which is difficult to achieve. c) Poleface windings often require a more complicated vacuum chamber. d) Poleface windings have to be securely attached to the poleface or vacuum chamber, which can be difficult if the poleface windings are exposed to strong radiation.

The method described here is closely related to poleface windings, but does not have the disadvantages mentioned above. What will be discussed are conductors that are imbedded in the iron. Since the effect of such windings is not nearly as simple as are the effects of poleface windings, we will make a series of qualitative considerations and simplified analytical calculations. They will give the understanding needed to design a functioning and efficient system. One of the simplifying assumptions made for this discussion is the restriction to homogeneous field magnets that are long in one (z) direction, so that only the two dimensional fields in the plane perpendicular to that direction (x-y-plane) need be considered. Generalizations are comparatively simple and will be briefly discussed.

Since it is the author's experience that some magnetic field problems are often more easily understood when discussed with the help of an Orthogonal Analog Model, this method will be used freely when appropriate. To make the paper self-contained, the validity of this model is proved, as are also some other elementary relations (e.g. the anisotropy properties of iron for perturbation effects). To avoid repeated interruption of the main arguments, these as well as most other mathematical derivations are put in appendices.

## 2. Units and Notation

With lengths measured in cm, currents in Ampères and both magnetic field quantities (B,H) measured in Gauss, current density $\vec{j}$ and field $\vec{H}$ are related through curl $\vec{H} = \mu_o \vec{j}$, with $\mu_o = .4 \cdot \pi$. The iron is assumed to be isotropic, and its properties are described by the dimensionless permeability $\mu = B/H$, or the reluctivity $\gamma = 1/\mu$. Unit vectors are represented by $\vec{e}$ with the appropriate subscript. Two dimensional fields are considered to be in the x-y-plane, and $\vec{B}$ can then be derived from a scalar potential V or a vector potential $\vec{A}$ which need to have only one component: $\vec{A} = \vec{e}_z A$. When fields are derived from the complex potential A + iV, we use the standard notation Z = x + iy (or w = u + iv), and the complex field quantity $B^* = B_x - i B_y$ is obtained from the complex potential F(Z) = A + iV through $B^* = i \, dF/dZ$.

## 3. Formulation of the Problem and its Basic Solution

Figure 1a shows the field line pattern in 1/4 of a windowframe magnet in and above the air gap and coil region. If the field in air is $\vec{B}_o$, and $\theta$ the angle between the normal to the air-iron interface and a field line in iron close to the interface, it follows from the continuity properties of $\vec{B}$ and $\vec{H}$ across an interface that the tangential field component $H_t$ at the interface is to very good approximation given by

$$H_t = B_o \cdot \gamma(B_o/\cos\theta) \cdot \mathrm{tg}\theta \quad . \tag{1}$$

Unless $\theta$ is sufficiently small, the dependence of $H_t$ on $\gamma$, which in turn depends very strongly on $B_o/\cos\theta$, leads to the undesirable field level dependent field distribution in the air region of the magnet. The effect of the tangential field component on the field in the air region is most easily seen by assuming $\mu = \infty$ for the iron and placing a current sheet at the interface with a sheet current density in the z direction of $I' = H_t\ \mu_o$(A/cm). ($I' > 0$ if the iron is to the left of the direction of $\vec{H}_t$.)

To get a feeling for the tolerable magnitude of $H_t$ and $\theta$, we assume that one can allow a sextupole contribution to the field whose relative field perturbation at the extreme aperture $x_o$ is $\delta$, i.e., we allow

$$H_y(x,o) = H_o \cdot (1 + \delta \cdot (x/x_o)^2) \quad . \tag{2}$$

Equation (A1.6) of appendix 1 gives the relation between $H_x$ off the midplane and $H_y$ in the midplane. If the halfgap of the magnet is h, eq. (A1.6) gives with eq. (2):

$$H_t = H_o \cdot 2\ \delta\ h\ x/x_o^2 \qquad (3)$$

Using this with eq. (1) gives

$$tg\theta = 2\ \mu\ \delta\ h\ x/x_o^2 \quad . \qquad (4)$$

Using the following representative numbers for a high resolution spectrometer: $\delta = 10^{-5}$; $x_o = 5h$; $\mu = 1000$ (1010 steel at 15 kG), at $x = x_o$ one obtains $\theta = 4.10^{-3}$. Looking at fig. 1a, it is obvious that, generally speaking, a windowframe magnet is intrinsically not suited for this type of application unless corrective measures are taken. It is also clear that even an H-magnet, where the sides of the pole can be shaped to get the field lines in the iron approximately perpendicular to the air-iron interface, will be very difficult to design to give the required small angles $\theta$.

To be able to make $H_t = 0$ at the interface, we propose to use conductors that are imbedded in the iron. Figure 1b shows the same magnet as the one depicted in fig. 1a, but with such conductors located in thin rectangularly shaped slots. The currents of the conductors have been optimized, and comparison of the fieldline patterns in figs. 1a and 1b shows immediately the drastic reduction of the above mentioned angle $\theta$.

Ignoring the rectangular slot for the moment, the field distribution produced by a filamentary conductor can be seen qualitatively by either thinking in terms of magnetic fields, or by using the orthogonal analog model (OAM) described in appendix 2. Using the latter method here, the conductor in the iron corresponds to a current fed into the conducting sheet. Considering field levels where $\gamma$ in the iron is small compared to its value (one) in air, the

resulting ratio of conductivities describing the air and iron region of the OAM leads to electric fields in the steel that are for all practical purposes perpendicular to the air-iron interface at that interface. In contrast to the pre-existing field produced by the conductors that are located in the air region, the magnetic field $\vec{B}$ produced by the conductor in the iron is therefore practically parallel to the air-iron interface at that interface. This fact has two consequences: 1) The conductor in the iron does produce a tangential field $H_t$ at the interface and therefore can be used to correct or cancel pre-existing tangential field components at the interface. This is the reason why we refer to the conductors in the iron as $H_t$-windings or conductors. 2) The fields produced in the iron by the $H_t$-conductor are for all practical purposes independent of the magnet gap, i.e., to obtain the tangential field component produced by the $H_t$-winding at the air-iron interface, one has to consider only the iron region of the magnet. The air region, and the placement of the main excitation currents in it, determine only the pre-existing field in the iron, i.e., the field with no current in the $H_t$-windings.

If one places a filamentary $H_t$-conductor into the iron, and assumes for the moment $\mu$ = constant, it is qualitatively clear that the $H_t$-distribution at the air-iron interface is a bell-shaped curve with a width of the order of the distance of the filament to the interface, and a peak value for $H_t$ of the order of the current divided by the width of the distribution.

The nonlinearity of the iron can modify this result significantly. Assuming a field level such that $\gamma$ increases with increasing field level, using the OAM, and refering to fig. 2, we can argue as follows: to the left of the filament $\vec{j}$ has the same direction as the pre-existing $\vec{j}$, whereas to the

right they have opposite directions. Because of the nonlinearity of the medium, the conductivity $\sigma$ goes up to the left of the filament, and down to the right. Consequently, more current flows to the left, and less to the right, etc. It is easy to see that something similar to a positive feedback is at work, and it is apparent that under these circumstances, the $H_t$-distribution would be significantly broadened, and its peak would move to the left.

The very strong fields in the vicinity of the $H_t$ conductor can be avoided by placing the conductor into a hole that has a large circumference. To avoid a strong perturbation of the fields by the void itself, it is advantageous to use a void of roughly rectangular shape, with the direction of the long dimension perpendicular to the interface. We thus have to understand the effect of the void itself, and the effect of the conductor in that void. But before discussing these two problems, we have to understand, at least to first order, how the nonlinearity of the iron modifies the effects of perturbations.

## 4. Modification of Perturbation Effects by the Nonlinearity of the Iron

To obtain the first order effects of a modification of a magnet, it is practical to express the modification in terms of a quantity that can be used as an expansion parameter for a Taylor series. In some cases the choice of the parameter is obvious, as for instance, when we want to find the effect of energizing a $H_t$ conductor. In other cases one has to generate the desired modification by introduction of an artificial parameter, such as the magnetic charges used below to create a void in the iron. For constant permeability the effects of charges or currents are easily evaluated by solving the field equations for the field perturbations because of the linearity of the magnetostatic equations in the field quantities, currents, and charges. The nonlinearity of the iron complicates this to a considerable extent.

Using current densities $\vec{j}_1$ and charges $q_1$ to describe the perturbations, introducing the perturbation size parameter $\varepsilon$ for bookkeeping purposes, describing the pre-existing fields and current densities by $\vec{B}_o$, $\vec{H}_o$, $\vec{j}_o$, and the field perturbations by $\vec{B}_1$, $\vec{H}_1$, the magnetostatic equations read: (the following is correct for the three dimensional case)

$$\text{div } \vec{B} = \text{div}(\vec{B}_o + \varepsilon \vec{B}_1) = \varepsilon q_1 \longrightarrow \text{div } \vec{B}_1 = q_1 \tag{5a}$$

$$\text{curl } \vec{H} = \text{curl}(\vec{H}_o + \varepsilon \vec{H}_1) = \vec{j}_o + \varepsilon \vec{j}_1 \longrightarrow \text{curl } \vec{H}_1 = \vec{j}_1 \tag{5b}$$

$$\vec{H} = \vec{H}_o + \varepsilon \vec{H}_1 = \gamma(|\vec{B}_o + \varepsilon \vec{B}_1|)\cdot(\vec{B}_o + \varepsilon \vec{B}_1) \tag{5c}$$

The relation between $\vec{H}_1$ and $\vec{B}_1$ to first order in $B_1$ is qualitatively clear: if $\vec{B}_1$ is parallel to $\vec{B}_o$, H changes by $H_1 = B_1 \cdot dH/dB$, whereas if $\vec{B}_1$ is in a direction perpendicular

to $\vec{B}_o$, the vector $\vec{B}$ is in linear approximation rotated without changing in amplitude, giving $H_1 = \gamma(B_o) \cdot B_1$. This is born out by an expansion of eq. (5c), carried out in appendix 3. The equations for the field perturbations are thus the normal magnetostatic equations in an anisotropic medium. The anisotropy of the steel for perturbation effects is a very strong one, as can be seen in fig. 3a, showing for a low carbon steel the permeability $\mu = B/H$, the differential permeability $dB/dH$, and the ratio of these "perturbation permeabilities", $\mu_\perp/\mu_\parallel = \gamma_\parallel/\gamma_\perp = d(\ell n\ H)/d(\ell n\ B)$, as a function of B. From the large value of $\gamma_\parallel/\gamma_\perp$ at high field levels follows that the $H_t$-distribution will be considerably broadened there compared to the isotropic case.

Because of the strong anisotropy of the iron for perturbations, we have to re-examine the boundary conditions in the iron at the iron-air interface: whereas in the isotropic case it is equivalent to state that $\vec{H}_1$ or $\vec{B}_1$ is parallel to the interface, this is clearly not the case with an anisotropic material. Considering the OAM, it is clear that $\vec{E}_1$ cannot have a tangential component at the interface, leading to the conclusion that in the iron $\vec{B}_1$ is the quantity that has to be parallel to the interface.

To acquire a semi-quantitative understanding of the effects of the anisotropy by performing some simple analytical calculations, it is reasonable to make some simplifying assumptions: in the region of interest the field has to be perpendicular to the air-iron interface for some distance, and should be homogeneous there. It is therefore a reasonable approximation to describe the iron for perturbation analysis purposes by an anisotropic medium with its axes parallel to the x- and y-axes, having field independent reluctivities $\gamma_x = H_o/B_o$ and $\gamma_y = d\ H_o/d\ B_o$ in these directions. The pertinent field

equations are derived and listed in appendix 4. The essential effect of the anisotropy for perturbations is that the y-coordinate axis appears stretched compared to the x-coordinate by the factor $\zeta^2 = (\gamma_y/\gamma_x)^{1/2}$ (fig. 3b). An illustrative example is the following: if a current filament is placed at distance $y_o$ above the straight air-iron interface of an otherwise unbounded medium, the $H_t$ distribution at the interface is the same that would be produced by a conductor placed at the distance $y_o \cdot \zeta^2$ in an isotropic medium.

5. Effect of a Void in the Iron

In order to find what $H_t$ is produced by an elongated slot in the presence of a previously homogeneous field $\vec{B}_o$ perpendicular to the interface, we take a two-step approach: we first describe the basic method used to generate a slot in an unbounded medium, and then consider the slot in a medium bound by a plane perpendicular to $\vec{B}_o$, calculate the $H_t$ there, and then the resulting $H_y$ in the air region.

Since we want to obtain only enough understanding of the effects of the slots to judge whether they do noticeable damage to the field in air, we are justified to make some simplifications. It is for instance qualitatively clear that the exact shape or length of the slot is not nearly as important as is its width.

From magnetic field or OAM considerations follows that for all practical purposes the boundary of the slot is an equipotential of A, i.e., a B-line. To generate a B-line of the desired shape in a pre-existing $\vec{B}_o = -\vec{e}_y \cdot B_o (B_o > 0)$, first we consider placing a magnetic line charge $q > 0$ at $x = 0$, $y = y_3 > 0$. Above that charge will be a point where the total field is zero, and at that point the field line coming from above splits into two parts, one going to the right and the other to the left, and then down. Needing to follow only the right branch for symmetry reasons, far enough down that line will be parallel again to $-\vec{e}_y$, but displaced to the right. Because of flux conservation, the ultimate displacement, i.e., the x-coordinate, of that line will be $q/2\ B_o$, independent of the nonlinearity of the iron. If we place a line charge $-q$ at $x = 0$, $0 < y = y_2 < y_3$, we create a slot with a halfwidth of a little less than $q/2\ B_o$, and a length of a little more than $y_3 - y_2$. From these

considerations it is clear that a first order perturbation calculation will give adequate information about $H_t$ at the interface. The boundary condition for the fields at the interface y = 0 is that $\vec{B}$ is tangential to the interface.

For symmetry reasons, $H_t$ is an odd function of x for a slot located on the y-axis. This means that $H_t$ can be significantly reduced by the presence of adjacent slots. Since in most cases one will use a number of equally spaced identical slots, the emphasis in the slot calculations in appendix 5 is on an infinite sequence of slots.

The essential conclusions from the calculations of the slot effects can be drawn from eqs. (A5.6) and (A5.9). The former describes the extreme value of $H_x$ at the interface produced by an infinitely long slot, and can be extrapolated to $x_1 \to \infty$, i.e., a single slot. In that case the last factor in eq. (A5.6) becomes one and the extreme value of $H_x$ depends only on the geometry and the regular reluctivity $\gamma = H/B$. For reasonably spaced slots, the last factor in eq. (A5.6) reduces the extreme values of $H_x$ significantly. At high field levels, where $\gamma_x$ is comparatively large, $\zeta^2$ is large also, helping strongly in making the second factor in eq. (A5.6) small. At lower field levels $\zeta^2$ becomes smaller, but $\gamma_x$ in general becomes quite small, so that with appropriate spacing of the slots the damaging effects can be kept at a tolerable level over a wide field range.

Similar comments apply to eq. (A5.9), describing the $H_y$-perturbation in the air region in terms of a Fourier series. For appropriate spacing of the slots, only the n = 1-term is significant. It should be noted that eqs. (A5.9) are not suited to describe only one slot. We do not describe the single slot effects in the air region since that case is relatively unimportant.

## 6. Effect of the Current in a Slot

We assume that the slot is long enough so that the feedback-like effect described in section 3 is not effective. We consider therefore the field perturbation produced by the $H_t$-current alone, (i.e., $\vec{B}_o = 0$), but take the pre-existing field into account by using an anisotropic medium, with the simplifications mentioned at the end of section 4.

To obtain a qualitative understanding of the effect of the $H_t$-current, we use again the OAM. The inside of the slot is then represented by a highly conducting medium, which is surrounded by an anisotropic medium. Taking the case of high field level, the conductivity in the direction of the pre-existing field (the x-direction in the OAM) will be higher than in the direction orthogonal to it, but still considerably lower than inside the slot.

The exception would be very high fields where $dH/dB \approx 1$. There one can dismiss the existence of the slot and need only to consider current filaments representing the conductors, without having to fear that the feedback-like effect occurs. Since the case $dH/dB \approx 1$ is relatively unimportant, we exclude it from the considerations below.

Because of the high conductivity of the slot, injection of current into the slot will cause a change of the scalar potential of the slot boundary relative to the air-iron interface ($y = 0$), which is assumed to be at $V = 0$. This means that the exact location of the conductor inside the slot is unimportant, and also that the width of the slot is of no consequence for the effect of the $H_t$-current. Consequently, the following model for the magnetic field calculation can be used: for $y = 0$ the vector potential A is set zero; the slot, extending from $y = y_2$ to $y = y_3$ ($x = 0$) is assumed to be infinitely thin and is put on a

constant vector potential $\neq 0$; the field equations for this model are solved in the u,v coordinate system introduced in appendix 4; the resulting $H_x$ is calculated and then integrated from $-\infty$ to $\infty$ to give the current that is associated with this solution. This calculation is carried out in appendix 6 and the result is eq. (A6.4). The bell-shaped $H_x$-distribution is broadened by a factor $\zeta^2$ because of the anisotropy of the iron for perturbations. For some calculations it is convenient to replace $y_2$ and $y_3$ by their arithmetic or geometric mean $\bar{y}$, giving the somewhat simpler Lorentz-shape for $H_x$: $H_x \sim (x^2 + (\zeta^2\,\bar{y})^2)^{-1}$ $(K(0) = \pi|2)$. This is usually of sufficient accuracy for $y_3/y_2 \leqslant 2$.

In deriving eq. (A4.4) the assumption has been made that the medium is bound only by the y = 0 line. Although one can introduce a number of refinements, they are not important enough to be reported here, with one exception: at the edge of an H-magnet, the air-iron interface turns up, and the effect of the $H_t$-winding closest to the edge can be significantly affected by this. This can be quite important since that is usually the $H_t$-conductor that requires the most current. For model calculations it would be somewhat complicated to deal with an actual $H_t$-winding slot. To get at least some idea about the effect of the edge, we therefore use the simpler model of a single $H_t$-current filament. Figure 6 shows the geometry for the model calculation. The pole contour is approximated in the x-y-system by the y = 0 line and the dashed line going to the left of the intersection point, and the location of the filament is indicated by the dashed arrow. To calculate the $H_t$ produced by the filament in this geometry, we follow the procedure used previously: we go into the u-v coordinate system. The new geometry, shown in fig. 6 for $\zeta^2 = 1.5$ is determined by the new left boundary, indicated by the solid line, and the transformed

location of the filament is indicated by the dotted arrow. The area bounded by the two solid lines is conformally mapped onto the upper half of a t-plane, the problem is solved there and the solution then used to extract the results of interest. The calculations are carried out in appendix 7, and for brevity, only the following conclusions are drawn: eq. (A7.4) gives a measure of the efficiency of an $H_t$-filament in the vicinity of the edge of the pole. It is directly evident how a large $\zeta^2$ makes the filament inefficient, unless it is reasonably far removed from the edge, i.e., $\alpha_1$ is sufficiently small. When judging the efficiency, one has to take the following into account: the outermost $H_t$ conductor will generally be placed a little outside the region where $H_t$-correction is necessary, i.e., one needs only about 40-50% of the total line integral over $H_t$ that is provided by the current, so that $\eta$ should be compared to about .5, and not 1. Equations (A7.5) and (A7.6) give $H_x(x,0)$, and the location of the maximum value of $H_x(x,0)$.

## 7. Design Considerations

Although the previous sections provide the basic body of information that is necessary to understand the important aspects of $H_t$-windings, it is difficult to derive from it hard rules about the design of $H_t$-winding systems. The reason is simply that so many parameters and considerations affect the problem that practically every system will be a compromise between magnetic requirements and mechanical considerations. Consequently, we can give only a brief listing of the general rules, guidelines and facts that should be considered when designing an $H_t$-winding system.

To design an $H_t$-system, one first has to obtain information about the amplitude, accuracy, and fine structure of the $H_t$ that needs to be generated. The main sources for the need of $H_t$-corrections will be saturation effects, necessity to be able to change the field distribution for beam optical reasons, and irregularities of the pole surface. Fortunately, the first two sources very seldom require detailed structure of the $H_t$-distribution. For a precision magnet it will always be necessary to have a well ground and polished surface of the poleface. Despite this, the assembled magnet will have field errors caused by non-parallelity of the polefaces, and warpage due to mechanical stresses. While it is of course important that these effects do not change with time after some initial aging effects, it is significant that again no detailed fine structure can be expected. The degree of fine structure of $H_t$ that one has to produce determines how narrow the bell-shaped $H_t$-distributions produced by the $H_t$-windings have to be, and the distance of the $H_t$-windings from the poleface should be such that that width of $H_t$-distribution is obtained for the largest value of $\zeta^2$ that will occur during operation of the magnet.

The lateral spacing of the $H_t$-windings should be such that the narrowest $H_t$-distributions, occurring at the field level giving the smallest value of $\zeta^2$, overlap sufficiently to allow production of the desired $H_t$-distribution with sufficient accuracy.

A good rule for the required spacing can be derived from the following simple model consideration: if one wants to represent the functions $g_o(x) = 1$ or $g_1(x) = x$ from $x = -\infty$ to $+\infty$ by a linear superposition of functions $(1 + x^2)^{-1}$ centered at locations $n \cdot \Delta x$, $n = -\infty$ to $\infty$, the error in fitting $g_o(x) = 1$ is $\pm 1/\cosh(2\pi/\Delta x)$, and for fitting $g_1(x) = x$, one has in addition to $\pm 1/\cosh(2\pi/\Delta x)$ a relative error of the same size. It follows that one would not want to have a spacing larger than the smallest half-amplitude width, and that it would seldom be worthwhile to use less than 1/2 of that.

To obtain a <u>rough</u> rule about the total $H_t$-winding current required, we make the following simple consideration: we consider $\int \vec{H} \cdot d\vec{s}$ along a closed path along the midplane from $x_1$ to $x_2$, up to the poleface ($y = h$), along the poleface, and back down to the starting point, and obtain: $\int_o^h (H_y(x_2,y) - H_y(x_1,y))dy = \int_{x_1}^{x_2} H_x(x,h)dx$. Applying this over a reasonably wide range in x, like one half of the total horizonatal aperture, equating the integral over $H_x$ with $\mu_o$ times the total $H_t$-winding current I in that range, we obtain approximately $\mu_o \cdot I \approx \Delta H_y \cdot h$. This estimate of the current gives remarkably low values for moderate correction requirements, but unfortunately it can seldom be used to estimate the $H_t$-current in the outermost conductor. There are two reasons for this: 1) As discussed in section 6, the conductor close to the outer boundary of the pole is used very inefficiently. 2) The $H_t$ has to be corrected not only in the useful aperture region, but also for some distance beyond the aperture, and $H_t$ tends to increase significantly in that region unless special precautions are taken.

To get some idea what an $H_t$-winding system is like, we give some numbers for a high resolution magnet that was designed recently. The dimensions of the aperture of 1/4 of the symmetrical magnet are: halfgap = 5 cm, usable horizontal half aperture = 32.5 cm. The poleface continues to about x = 40 cm, and then goes up with an angle of 52°. The corner is appropriately rounded, and the region of the pole beyond the aperture has been shimmed to give relative field errors of less than $10^{-5}$ inside the aperture for infinite permeability. In the first quadrant, four $H_t$ slots of .5 cm width are placed that extend from 3.75 cm to 7.5 cm above the poleface and are located at x = 5 cm, 15 cm, 25 cm, 35 cm. Evaluation of the field with a magnet analysis program with field dependent permeability at 14 kG gave a field inhomogeneity of $26 \cdot 10^{-5}$. Optimization of the $H_t$ currents with a program that is a combination of the analysis program and an optimization program[2]) gave for the $H_t$ conductors the currents 12.2A, -7.8A, 34.8A, -744A, giving a field homogeneity of $2 \cdot 10^{-5}$. For the conductor located at x > 25 cm, the width of the $H_t$-distribution was compared with the width calculated from the model discussed above, giving good agreement. To obtain a homogeneous field with a sextupole added whose relative field contribution was .2% at x = 32.5 cm gave (again at 14 kG) for the currents -39A, -50A, -105A, -877A, and the desired field distribution was produced with a relative error of $10^{-5}$. The rough rule given above to estimate the current in the conductors holds reasonably well for the first three conductors, but, as expected, fails miserably for the last conductor. It also follows from the numbers given here that, generally speaking, $H_t$-windings are a very good tool to make a good magnet extremely good, but are not suited to make a poor magnet good, or to produce strong harmonics. One

additional comment to the numbers given above is in order: while the magnet analysis code does not have an absolute accuracy of $10^{-5}$, its self-consistent accuracy is considerably better. Therefore the quoted currents will be roughly correct, but for an actual magnet they will be slightly different and should be determined by making measurements of the field errors and of the effect of the individual conductors, and then using an optimization procedure like that described in ref. [2]) to determine the correct $H_t$-winding excitations.

To summarize the essential design steps, the following procedure has proved useful: 1) Estimate (possibly aided by a magnet analysis program) of amplitude and fine structure of $H_t$ to be provided. 2) Preliminary design of slot and conductor system consistent with the requirement that the slots are realizable (see below) and cause tolerable field distortions. 3) Optimization of correction currents at field levels of interest, using the $H_t$-distributions caused by currents derived in the appendices. 4) Optimization of currents with magnet analysis and optimization program.

The difficulty of creating the slots for the conductors depends strongly on the details of the magnet construction. It is for instance easy to punch appropriate holes into the sheets comprising a laminated magnet. For a solid core high precision magnet it is always advisable to use a poleface plate of high quality steel. The back side is then accessible for machining purposes. While it is relatively easy to produce narrow and deep slots in a straight magnet, this is more difficult for a curved bending magnet. The solution chosen for the magnet discussed above is the following: 1 cm wide slots will be machined, but will then be partially filled with iron on one side and the top to obtain the desired slot geometry.

It is impossible to establish general rules how the $H_t$ conductors should be fed since too many details of the construction of the magnet influence that choice. If each conductor is individually fed, one can let it penetrate the end, side, or top of the magnet. If one wants to feed pairs of conductors in a magnet half with currents that are equal in amplitude, but with opposite signs, one can close the loop in the iron and then feed it coaxially from one side or the top.

Energizing the conductors should in general not be too expensive. If it is necessary to have control over the field shape during routine operation, appropriate power supplies are needed. Since the power dissipation in the $H_t$-windings is extremely small compared to the main coils, and since the current stabilization requirements are less stringent, the $H_t$-power supplies should cost only a small fraction of the main power supply. If, after initially establishing the relation between the $H_t$-currents and the main excitation currents, the $H_t$-currents will always be operated according to this relationship, one can energize the $H_t$-windings from the main power supply with appropriate auxiliary circuits to obtain the nonlinear relation between the currents.

Since one wants to go only once through the exercise of establishing the $H_t$-currents at the various field levels, it is imperative that the magnetic field is reproducible. It is therefore advisable to go always through the same magnetic cycle, i.e., the magnet should always go from zero field to the top field, then back to zero field, etc. If the magnet is not laminated, large field level changes have to be produced in such a way that DC aftereffects resulting from eddy currents are sufficiently suppressed[5]). From the mechanical

point of view, small deformations with field level are permissible, since they will also be present when the $H_t$-currents are optimized with the help of measurements. But these deformations should be reproducible.

## 8. Generalizations

Since in all previous sections it has been assumed that the magnet and the correction field has midplane symmetry, it has to be stated that use of that simplification was a matter of convenience, not necessity. It is furthermore clear that although we discussed exclusively homogeneous field magnets, $H_t$-windings can be used for other magnets as well. Since it is obviously impossible to list all conceivable applications, only some basic rules will be discussed.

When dealing with a two dimensional magnet such as a multipole magnet or a strong focusing bending magnet, designed to produce a non-uniform field, the desired field distribution will be known. Consequently, the complex potential describing that field is also known, and it is directly proportional to the conformal transformation that maps the idealized polefaces of the magnet onto straight lines, i.e., the transformation that transforms the inhomogeneous field magnet into a homogeneous field magnet. The concepts developed here can therefore be applied, and the resultant configuration then be transformed back into the real magnet geometry. The effects arising from dealing with nonlinear iron in transformed geometry[6]) will in most cases be so small that it will not be necessary to change the basic design of the system. It is worthwhile to note that it might be advantageous to optimize the poleface of an inhomogeneous field magnet to give the desired field distribution at the highest field level. If that is done, the $H_t$-windings need to be energized only at intermediate and low field levels, leading to a reduction of the largest $H_t$-currents. While this procedure does not lead to additional expense in producing the polefaces, since they are non-planar anyway, it would make the production of the poleface of a homogeneous field magnet more expensive in most cases.

The considerations in this paper have been purely two dimensional. But it is clear that $H_t$-windings can also be useful for three dimensional configurations, and the concepts developed here will give at the very least a good starting point for the design of such systems.

## Appendix 1. Some Relationships Between Field Components in the Aperture Region of Dipole Magnets

To obtain a relationship between $H_y$ in the midplane and $H_x$ off the midplane of a homogeneous field magnet, we apply a Fourier transform over x to the magnetostatic equations

$$\partial H_x/\partial x + \partial H_y/\partial y = 0 \quad . \tag{A1.1a}$$

$$\partial H_y/\partial x - \partial H_x/\partial y = 0 \quad . \tag{A1.1b}$$

With

$$\mathcal{H}(p,y) = \int_{-\infty}^{\infty} H(x,y)e^{-px}\,dx$$

we obtain

$$p\mathcal{H}_x + \partial\mathcal{H}_y/\partial y = 0 \tag{A1.2a}$$

$$p\mathcal{H}_y - \partial\mathcal{H}_x/\partial y = 0 \quad . \tag{A1.2b}$$

For this transformation to be valid, one has to assume, at least in principle, that the air region between the polefaces at $y = \pm h$, extends in the x direction from $-\infty$ to $+\infty$. Since this condition is not of too much importance for our purposes, and since it can also be eliminated, it will not be discussed further.

Eliminating $H_y$ with eq. (A1.2b), we obtain

$$\partial^2\mathcal{H}_x/\partial y^2 + p^2\mathcal{H}_x = 0 \quad ,$$

and the solution

$$\mathcal{H}_x(p,y) = \sin(py)\cdot f(p) \quad . \tag{A1.3}$$

The other integration constant is zero, since $H_x(x,0) \equiv 0$ for symmetry reasons. Using eq. (A1.3) in eq. (A1.2b), we obtain

$$\mathcal{H}_y(p,y) = \cos(py)\cdot f(p) \quad .$$

Setting $y = y_1$ in the last equation gives for eq. (A1.3)

$$\mathcal{H}_x(p,y) = \mathcal{H}_y(p,y_1)\cdot \sin(py)/\cos(py_1) \quad . \tag{A1.4}$$

For $y_1 = 0$ we obtain

$$\mathcal{H}_x(p,y) = \sin(py)\cdot \mathcal{H}_y(p,0) \quad . \tag{A1.5}$$

Taking the inverse Fourier transform of this equation yields

$$H_x(x,y) = \sin(y\partial/\partial x)\cdot H_y(x,0) = \sum_{n=0}^{\infty} (-1)^n \frac{(y\partial/\partial x)^{2n+1}}{(2n+1)!} H_y(x,0) \quad . \tag{A1.6}$$

If one wants to express $H_y(x,0)$ in terms of $H_x(x,y)$, one can solve eq. (A1.5) for $\mathcal{H}_y(p,0)$, and apply the inverse Fourier transform, giving

$$H_y(x,0) = \int_{-\infty}^{\infty} H_x(x',y)\cdot \tanh\left(\frac{\pi}{2}\cdot\frac{x-x'}{y}\right)\cdot dx'/2y \quad . \tag{A1.7}$$

For completeness it should be mentioned that eq. (A1.7) gives only the $H_y(x,0)$ due to $H_x(x,y)$, i.e., one can add to the right side of eq. (A1.7) any solutions

to the magnetostatic equations that satisfy the symmetry of the problem and have $H_x(x',y) \equiv 0$. One obvious such function is the constant describing a perfectly homogeneous field.

## Appendix 2. The Orthogonal Analog Model

It is often convenient to get an understanding of two dimensional magnetic field distributions by considering current and field distributions in an orthogonal analog model (OAM). The pertinent relationships are derived here since this OAM is not as widely known as one would expect, considering the fact that it has been used in the past to make model measurements[4]).

The OAM consists of a very thin conducting sheet with a location and field dependent electric conductivity. Into the sheet one feeds from the third dimension a current density that is equivalent to the current density that excites the magnet. To get the equivalences, we write down the magnetic and electric equations in such a way that the equivalences become obvious.

Deriving $\vec{B}$ from the vector potential $\vec{A} = \vec{e}_z \cdot A$, one obtains

$$\vec{B} = \text{curl}(A\,\vec{e}_z) = \text{grad}A \times \vec{e}_z \qquad \text{(A2.1a)}$$

$$\vec{H} = \gamma\,\vec{B} = \gamma\ \text{grad}A \times \vec{e}_z \qquad \text{(A2.1b)}$$

$$\text{curl}\,\vec{H} = -\vec{e}_z \cdot \text{div}(\gamma\ \text{grad}A) = \vec{e}_z \cdot \mu_o\, j_z$$

$$\text{div}(\gamma\ \text{grad}A) = -\mu_o\, j_z \quad . \qquad \text{(A2.1c)}$$

We derive the electric field $\vec{E}$ in the conducting sheet from a scalar potential V, and obtain then from $\vec{E}$ and the conductivity $\sigma$ the two dimensional current density $\vec{j}$.

$$\vec{E} = -\text{grad}V \qquad \text{(A2.2a)}$$

$$\vec{j} = \sigma \vec{E} = -\sigma \, \text{grad}V \quad . \tag{A2.2b}$$

In calculating the divergence of the three dimensional current density, the contribution $\partial j_z/\partial z$ from the current density that is fed into the sheet from the third dimension can be replaced by $j_z/d$, where d is the thickness of the sheet. One thus obtains from charge conservation

$$-\text{div}\, \vec{j} = \text{div}(\sigma \, \text{grad}V) = j_z/d \quad . \tag{A2.2c}$$

Comparing the two sets of eqs. (A2.1) and (A2.2), they are identical if one introduces the following equivalences:

| | | | | | |
|---|---|---|---|---|---|
| A | $\vec{B}$ | $\vec{H}$ | $\gamma$ | $\mu_o j_z$ | Magnet |
| $\updownarrow$ | $\updownarrow$ | $\updownarrow$ | $\updownarrow$ | $\updownarrow$ | |
| V | $\vec{e}_z \times \vec{E}$ | $\vec{e}_z \times \vec{j}$ | $\sigma$ | $-j_z/d$ . | OAM |

(A2.3)

It is apparent from this derivation that the OAM is also valid for anisotropic media.

## Appendix 3. Relationship Between Perturbation Fields $\vec{H}_1$ and $\vec{B}_1$ for Nonlinear Isotropic Steel

To first order in $\varepsilon$, one obtains with $B = |\vec{B}| = (B_o^2 + 2\varepsilon \vec{B}_o \cdot \vec{B}_1)^{1/2}$, $\gamma_o' = (dH/dB)_{B=B_o}$, and $\gamma_o = \gamma(B_o)$:

$$\vec{H}_o + \varepsilon \vec{H}_1 = (\gamma_o + \varepsilon \gamma_o' \vec{B}_1 \cdot \vec{B}_o/|B_o|)(\vec{B}_o + \varepsilon \vec{B}_1)$$

$$\vec{H}_1 = \gamma_o \vec{B}_1 + \gamma_o' \vec{B}_o \cdot \vec{B}_1 (\vec{B}_o/|B_o|) \quad .$$

Indicating unit vectors and field components parallel and perpendicular to $\vec{B}_o$ by the subscripts $\parallel$ and $\perp$, we obtain:

$$\vec{H}_1 = \vec{e}_\parallel (\gamma_o' B_o B_{1,\parallel} + \gamma_o B_{1,\parallel}) + \vec{e}_\perp B_{1,\perp} \gamma_o \quad .$$

With $\gamma_o' B_o + \gamma_o = (B_o \gamma_o)' = dH_o/dB_o$, $\vec{H}_1$ becomes:

$$\vec{H}_1 = \vec{e}_\parallel \cdot B_{1,\parallel} \cdot dH_o/dB_o + \vec{e}_\perp \cdot B_{1,\perp} \gamma_o \quad .$$

## Appendix 4. Description of Magnetic Fields in Linear Anisotropic Steel

Deriving $\vec{B}$ from the vector potential A through

$$\vec{B} = \text{curl } \vec{A} \tag{A4.1a}$$

$$B_x = A'_y ; \; B_y = -A'_x \quad , \tag{A4.1b}$$

$\vec{H}$ becomes in an anisotropic medium with field and location independent reluctivities $\gamma_x$, $\gamma_y$ in the x- and y-directions

$$H_x = \gamma_x A'_y ; \; H_y = -\gamma_y \cdot A'_x \quad , \tag{A4.2}$$

and curl $\vec{H} = \mu_o \vec{j}$ gives

$$\gamma_y A''_{xx} + \gamma_x A''_{yy} = -\mu_o j \quad . \tag{A4.3}$$

Introducing

$$\overline{\gamma} = 1/\overline{\mu} = (\gamma_x \gamma_y)^{1/2} \tag{A4.4a}$$

$$\zeta = (\gamma_y/\gamma_x)^{1/4} \tag{A4.4b}$$

$$u = x/\zeta \quad , \quad v = y \cdot \zeta \quad , \tag{A4.4c}$$

eq. (A4.3) becomes

$$A''_{uu} + A''_{vv} = -\mu_o \overline{\mu} j \quad .$$

Since the Laplace operator occurs on the left side of this equation, A must be a harmonic function of u and v where j = 0. Consequently, the normal apparatus for deriving fields from a complex potential can be used in the u-v coordinate system, and we have to list only some definitions and expressions for the fields:

$$w = u + iv$$

$$F(w) = A + iV$$

$$B_w^* = B_u - i\,B_v = i\,dF/dw \tag{A4.5a}$$

$$B_x = B_u \cdot \zeta \tag{A4.5b}$$

$$B_y = B_v/\zeta \tag{A4.5c}$$

$$H_x = B_u \cdot \bar{\gamma}/\zeta = B_u \cdot \gamma_x\,\zeta = -\bar{\gamma}\,V'_x \tag{A4.5d}$$

$$H_y = B_v\,\bar{\gamma}\,\zeta = B_v\,\gamma_y/\zeta = -\bar{\gamma}\,V'_y \quad . \tag{A4.5e}$$

The last part of the last two equations means that, in normal x-y-coordinate system notation, $\vec{H}$ can be expressed as

$$\vec{H} = -\bar{\gamma}\,\mathrm{grad}V \quad . \tag{A4.5f}$$

The complex potential F(w), describing the fields resulting from a current filament at w = 0, in an unbounded medium, is given by

$$F(w) = -\frac{\mu_o\,\bar{\mu}\,j}{2\pi}\ln(w) = -\frac{\mu_o\,\bar{\mu}\,j}{2\pi}\left(\frac{1}{2}\ln(u^2 + v^2) + i\,\mathrm{arctg}(v/u)\right) \quad .$$

The lines of constant vector potential are therefore given by

$u^2 + v^2 = (\frac{x}{\zeta})^2 + (\zeta y)^2 = \text{const}$, i.e., the B-lines are ellipses in the x-y-coordinate system. Similarly, lines of constant scaler potential are $v/u = \zeta^2\, y/x = \text{const}$, i.e., the H-lines are circles in the x-y-coordinate system.

## Appendix 5. Field Perturbations Caused by Slots in the Steel

The calculations to obtain the effect of slots are done in the u-v system, using the same subscripts as in the x-y system.

If the slots of a periodic series of slots are separated by $2u_1$, we need to consider only the fields in the area outlined in fig. 4, with the boundary conditions that the field $\vec{B}$ caused by the perturbation is tangential to the boundaries. To do this, we first map conformally the outlined region onto the upper half of a t-plane with a Schwarz-Christoffel transformation.

$$dw/dt = c/(1 - t^2)^{1/2}$$

$$w = c \cdot \arcsin(t)$$

$$u_1 = c \cdot \pi/2$$

$$t = \sin(\pi w/2u_1) \quad . \qquad \text{(A5.1)}$$

Since the pre-existing field in the u-v system is $\zeta B_o$ (eq. (A4.5c)), the charges q needed to create a slot with a width $2u_o (<< 2u_1)$ are then equal $\pm\zeta B_o \cdot 2u_o$. The perturbation potential $F_1$ that has singularities corresponding the charges placed at $w = i v_2$, $i v_3$, and giving constant vector potential along the boundary is then given by

$$F_1 = \zeta B_o \cdot \frac{i\, 2u_o}{2\pi} \left(\ln(t - t_2)(t - t_2^*) - \ln(t - t_3)(t - t_3^*)\right) \quad .$$

Combining this with the complex potential describing the pre-existing field, using eq. (A5.1) and the identity $\sin^2\alpha + \sinh^2\beta = (\cosh 2\beta - \cos 2\alpha)/2$ gives with

$$\alpha = \pi\, w/u_1 \quad , \quad \beta_{2,3} = \pi \cdot v_{2,3}/u_1 :$$

$$F(w) = \zeta\, B_o (w + i\, \frac{u_o}{\pi} \{\ln(\cosh\beta_2 - \cos\alpha) - \ln(\cosh\beta_3 - \cos\alpha)\}) \tag{A5.2}$$

$$B_w^* = \zeta\, B_o (i - \frac{u_o}{u_1} \cdot \sin\alpha \{(\cosh\beta_2 - \cos\alpha)^{-1} - (\cosh\beta_3 - \cos\alpha)^{-1}\}) \quad . \tag{A5.3}$$

To get the exact intersections of the slot with the v axis, one has to solve $B_w^* = 0$. Since Re $F(0) = 0$, the exact shape of the slot, and from it its exact width, is obtained from Re $F(w) = 0$. However, for a reasonably long slot with a width $<< 2u_1$, the approximate coordinates $v_2$, $v_3$ for the ends and the value $2u_o$ for the width are sufficiently accurate and will be used.

To get $H_t$ at the interface in the x-y-system, we apply eqs. (A4.4) and (A4.5) to eq. (A5.3) and obtain with

$$\alpha = \pi x/x_1 \quad , \quad \beta_{2,3} = \zeta^2\, \pi\, y_{2,3}/x_1 :$$

$$H_x/B_1 = -\gamma_x\, \zeta^2 \cdot \frac{x_o}{x_1} \sin\alpha \{(\cosh\beta_2 - \cos\alpha)^{-1} - (\cosh\beta_3 - \cos\alpha)^{-1}\} \quad . \tag{A5.4}$$

To obtain a better feeling for $H_x$, we drop for simplicity the second term in the bracket of eq. (A5.4), i.e., assume an infinitely long slot, and find the maximum of

$$f(\alpha) = \sin\alpha/(\cosh\beta_2 - \cos\alpha) \quad . \tag{A5.5}$$

It occurs for $\cos\alpha = 1/\cosh\beta_2$. $f(\alpha)$ has there the value $1/\sinh\beta_2$, giving for the extreme value of $H_x/B_o$:

$$(H_x/B_o)_{Extr.} = -\gamma_x \cdot \frac{x_o}{\pi\, y_2} \cdot \frac{\zeta^2\, \pi\, y_2/x_1}{\sinh(\zeta^2\, \pi\, y_2/x_1)} \quad . \tag{A5.6}$$

To obtain $H_y$ in the air region, it is convenient to expand $f(\alpha)$ into a Fourier series:

$$f(\alpha) = \sum_{-\infty}^{\infty} a_n\, e^{in\alpha} \quad . \tag{A5.7}$$

The coefficients $a_n$ are easily evaluated, giving for a finite length slot

$$a_o = 0;\ n > 0:\ a_n = -i(e^{-n\beta_2} - e^{-n\beta_3});\ a_{-n} = a_n^* \quad . \tag{A5.8}$$

Using eq. (A1.4) to obtain the transfer function of the Fourier series that relates $H_y$ at location y above the midplane of the air region to $H_x$ at the air-iron interface (h = half gap of the air region) gives

$$H_y(x,y)/B_o = \sum_{1}^{\infty} b_n \cos(n\, \pi\, x/x_1) \quad , \tag{A5.9a}$$

$$b_n = \gamma_x \cdot \zeta^2 \cdot \frac{2x_o}{x_1} (\exp(-n\zeta^2\, \pi\, y_2/x_1) - \exp(-n\zeta^2\, \pi\, y_3/x_1)) \tag{A5.9b}$$

$$x\, \cosh(n\, \pi\, y/x_1)/\sinh(n\, \pi\, h/x_1) \quad .$$

## Appendix 6. Fields Produced by a Conductor in a Thin Slot

For symmetry reasons, the problem specified in section 6 needs to be solved only for $u > 0$. The geometry is shown in fig. 5a, and the first quadrant of the w-plane is conformally mapped onto the upper half of a t-plane with a Schwarz-Christoffel transformation:

$$dw/dt = .5\ t^{-1/2} \tag{A6.1}$$

$$w = t^{1/2} \quad ; \quad t = w^2 \quad . \tag{A6.2}$$

Figure 5b shows the map of the boundary of the first quadrant of the complex w-plane onto the complex potential plane F(w). The differential equation for the Schwarz-Christoffel transformation that maps the inside of the rectangle in fig. 5b onto the upper half of the t-plane is

$$dF/dt = -i\cdot 0.5\cdot c_1\cdot(t(t - t_2)(t - t_3))^{-1/2} \quad . \tag{A6.3}$$

Integration of this equation is not necessary since we are only interested in $B_w^* = i\ dF/dw$, which is directly obtained from eqs. (A6.1), (A6.3), and (A6.2):

$$B_w^* = c_1((t - t_2)(t - t_3))^{-1/2} = c_1((w^2 + v_2^2)(w^2 + v_3^2))^{-1/2} \quad .$$

Introducing now the x and y coordinates with eq. (A4.4), and a new constant $c_2$, gives for $H_x$:

$$H_x(x,0) = c_2((x^2 + (\zeta^2\ y_2)^2)(x^2 + (\zeta^2\ y_3)^2))^{-1/2} \quad . \tag{A6.4a}$$

Using this expression now over the whole x-axis and normalizing with $\int_{-\infty}^{\infty} H_x(x,0)\,dx = \mu_o I$ gives for $c_2$ (K represents the complete elliptic integral of the first kind):

$$c_2 = .5\,\mu_o\, I\cdot\zeta^2\, y_3/K(1 - y_2^2/y_3^2) \quad . \qquad \text{(A6.4b)}$$

## Appendix 7. Effect of Conductor Imbedded in the Steel Close to the Edge of a Pole Piece

Transforming the x-y geometry into the u-v geometry gives with fig. 6 and eq. (A4.4c):

$$tg\alpha_2 = \zeta^2\, tg\alpha_1 \quad ; \quad tg\beta_2 = \zeta^2\, tg\beta_1 \quad , \tag{A7.1a}$$

$$|w_2|^2 = x_2^2/\zeta^2 + y_2^2\, \zeta^2 \quad . \tag{A7.1b}$$

The expression that gives the Schwarz-Christoffel transformation that conformally maps the area bound by the solid lines onto the upper half of a t-plane can be written as

$$dw/dt = (1 - n)t^{-n} \quad ; \quad n = \beta_2/\pi \quad , \tag{A7.2a}$$

giving

$$w = t^{1-n} \quad ; \quad t = w^a \quad ; \quad a = 1/(1 - n) \quad . \tag{A7.2b}$$

The complex potential F that has a singularity at $t_2 = w_2^a$ corresponding to a current filament there, and a constant vector potential along the real t-axis, i.e., on the problem boundary, is given by

$$F = - \frac{\mu_o \bar{\mu}\, I}{2\pi} \ln\left(\frac{t - t_2}{t - t_2^*}\right) \quad . \tag{A7.3}$$

The line integral of $H_t$ along the total problem boundary in the x-y-geometry equals $I\, \mu_o$. To judge the efficiency $\eta$ of the filament, we calculate what

fraction $\eta \cdot I \cdot \mu_o$ of that line integral is contributed from the integral of $H_t$ along the real x-axis. $\eta \cdot I\ \mu_o$ is obviously given by $\bar{\gamma}$ times the difference of the imaginary part of F between the points t = 0 and $t \to \infty$. From eqs. (A7.2b) and (A7.3) one obtains:

$$\eta = ((\pi - \beta_2) - \alpha_2)/(\pi - \beta_2) \quad . \tag{A7.4}$$

To obtain $H_x$, we first calculate $B_w^* = i(dF/dt)/(dw/dt)$. With eqs. (A7.2a) and (A7.3) we obtain:

$$B_w^* = -i\,\frac{\mu_o\,\bar{\mu}\,I\,a}{2\pi} \cdot \frac{(t_2 - t_2^*)t^n}{t^2 - t(t_2 + t_2^*) + t_2\,t_2^*} \quad .$$

From this follows with eqs. (A7.2b) and (A4.5d) for $H_x$:

$$\left.\begin{aligned} H_x &= \frac{\mu_o\,I\,a}{\pi\,\zeta^2|w_2|} \cdot \frac{s^n \cdot \sin(a\alpha_2)}{s^2 - 2s\cdot\cos(a\alpha_2) + 1} \\ s &= (x/\zeta|w_2|)^a \end{aligned}\right\} \tag{A7.5}$$

The maximum for $H_x$ occurs at

$$s = ((1 - n)\cdot\cos(a\alpha_2) + (1 - (1 - n)^2 \sin^2(a\alpha_2))^{1/2})/(2 - n) \quad . \tag{A7.6}$$

## References

1) G. Bronca et al., L'Onde electrique 39 (1959) 463

2) K. Halbach, Proc. Internat. Conf. on Magnet Technology, Oxford, 1967, p. 47; University of California, Lawrence Radiation Laboratory Report UCRL-17436 (1967)

3) M. S. Livingston and J. P. Belwett, Particle Accelerators, McGraw-Hill, 1962, p. 462

4) Asner et al., Proc. Internat. Conf. on Magnet Technology, Stanford, 1965, p. 126

5) K. Halbach, UCRL Report 18969, to be published in Nucl. Instr. Methods

6) K. Halbach, Nucl. Instr. Methods 64 (1968) 278

## Figure Captions

Fig. 1a. Fieldline pattern in part of a windowframe magnet, without $H_t$-conductors.

b. Fieldline pattern in part of a windowframe magnet, with $H_t$-conductors.

Fig. 2. Schematic $H_t$-conductor fields in OAM.

Fig. 3a. B/H, dB/dH, and dlnH/dlnB vs. B.

b. $(\mathrm{dlnH/dlnB})^{1/2}$ vs. B.

Fig. 4. Geometry for evaluation of slot effect.

Fig. 5. Geometry for evaluation of $H_t$-conductor effect.

Fig. 6. Geometry for evaluation of pole edge effect.

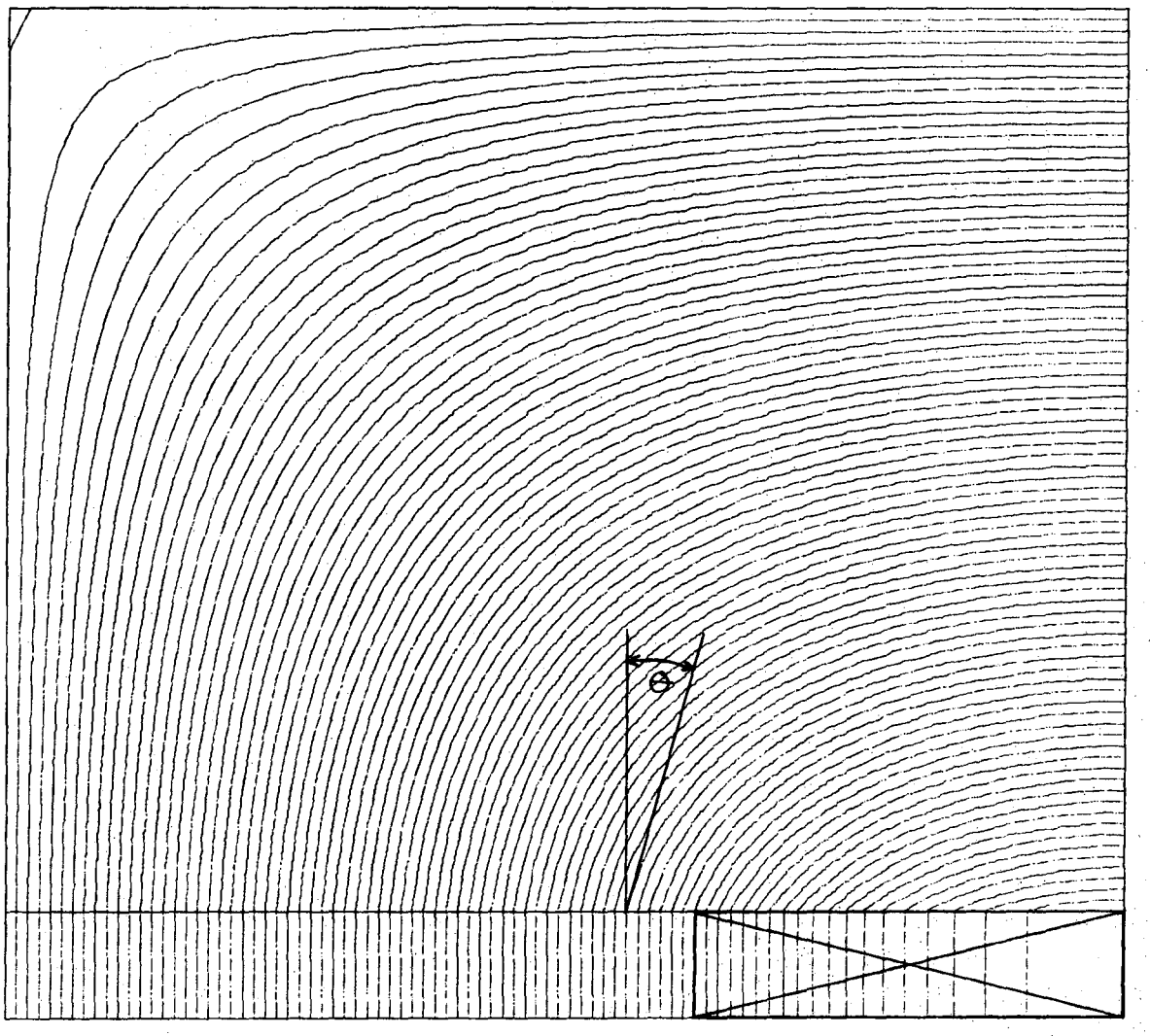


XBL 7210-1991

Fig. 1A

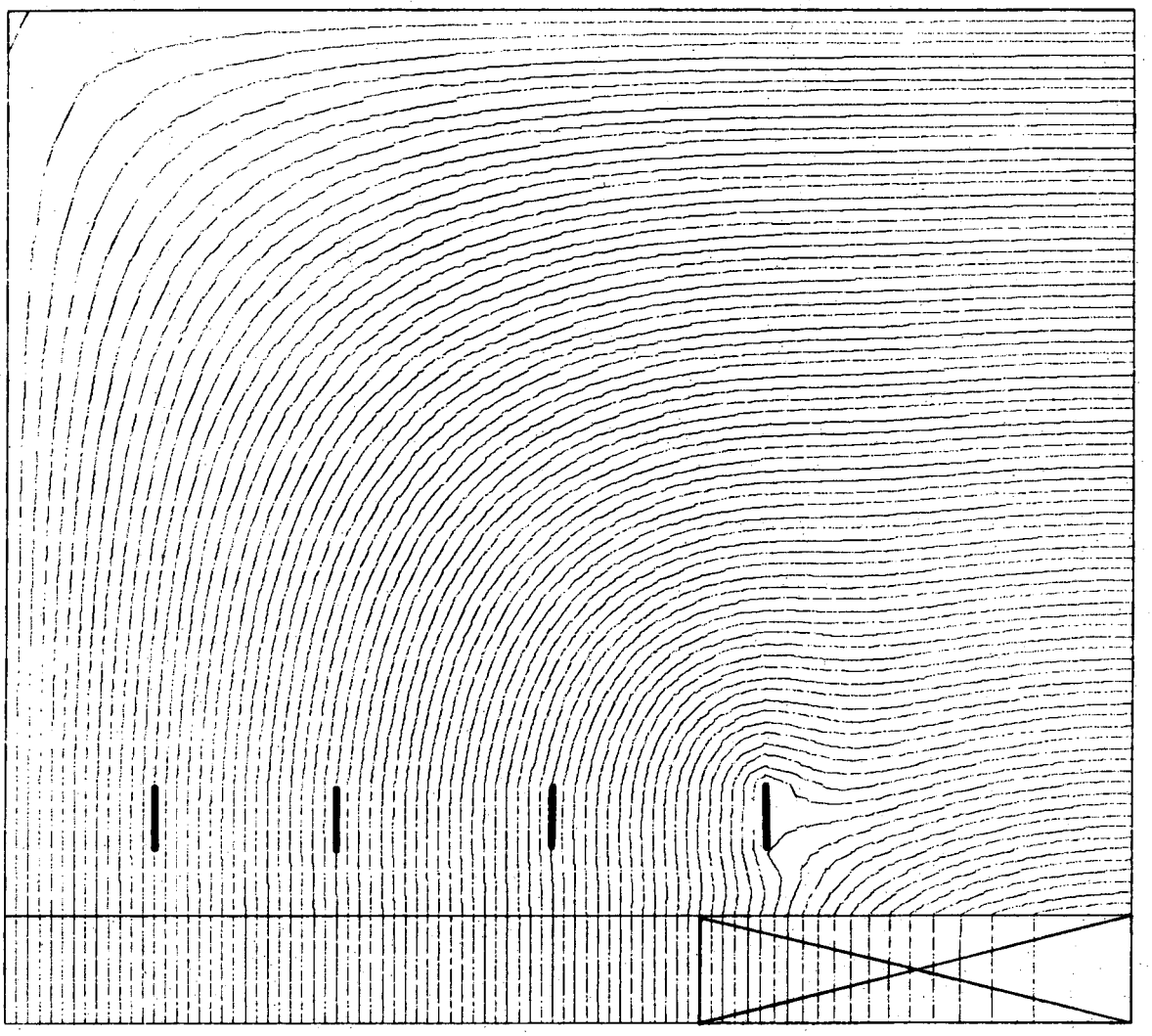

XBL 7210-1999

Fig. 1B

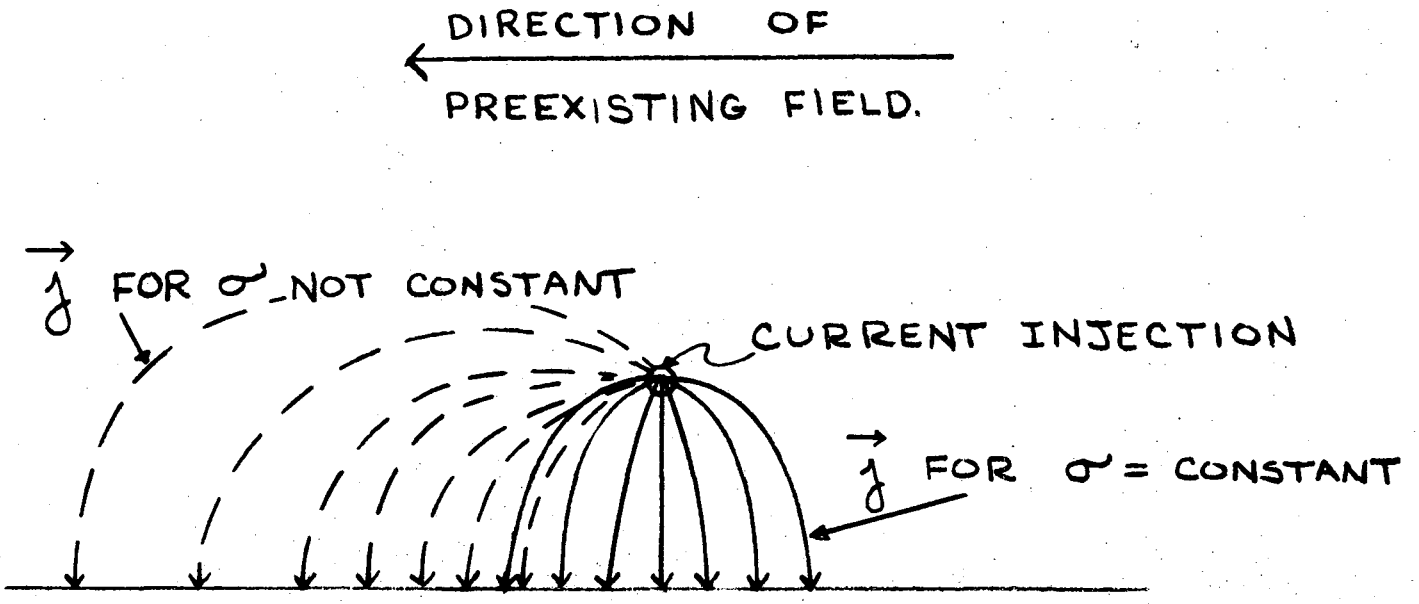


FIG. 2

XBL 7210-1990



UCRL-18969

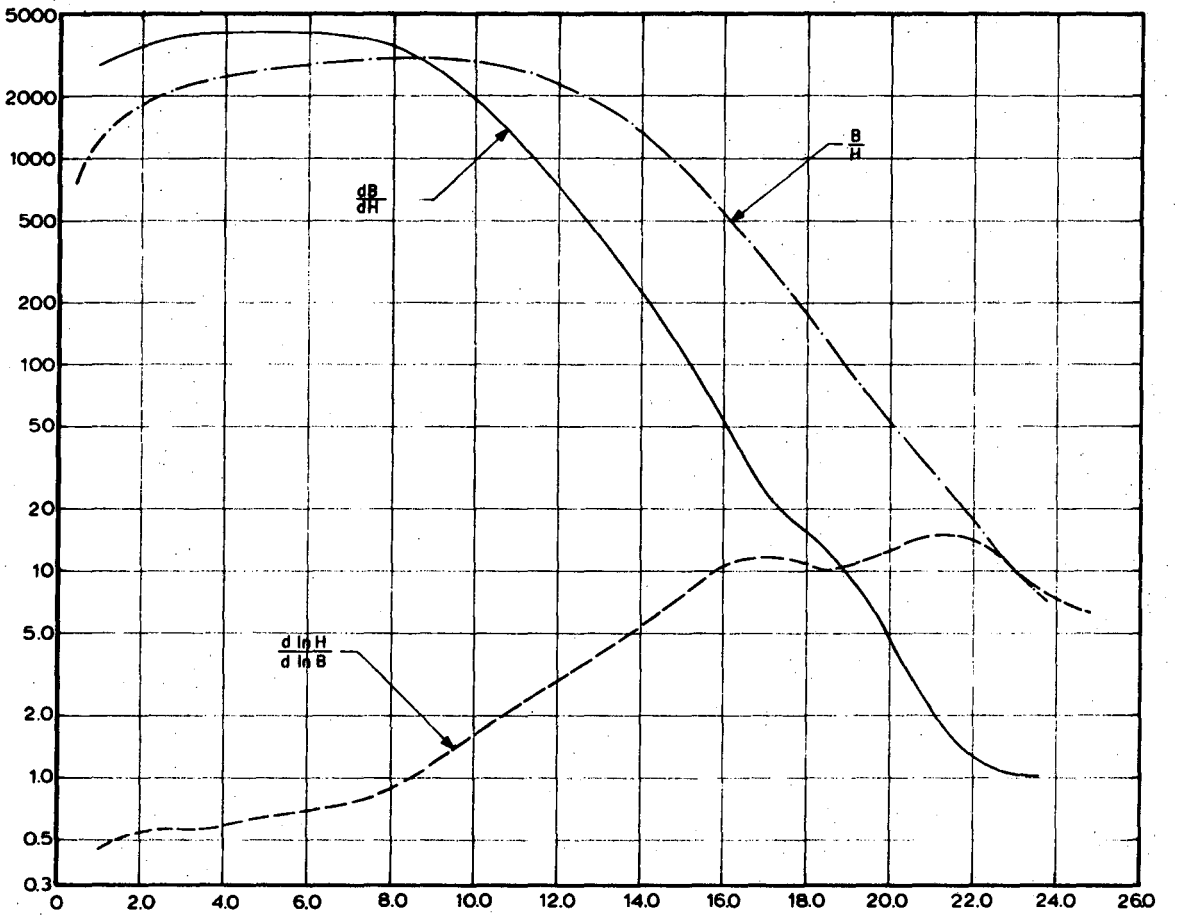
5000
2000
1000
500
200
100
50
20
10
5.0
2.0
1.0
0.5
0.3
0
2.0
4.0
6.0
8.0
10.0
12.0
14.0
16.0
18.0
20.0
22.0
24.0
26.0
dB/dH
B/H
d ln H / d ln B
B – kilogauss
XBL 7012 6270

Fig. 3A

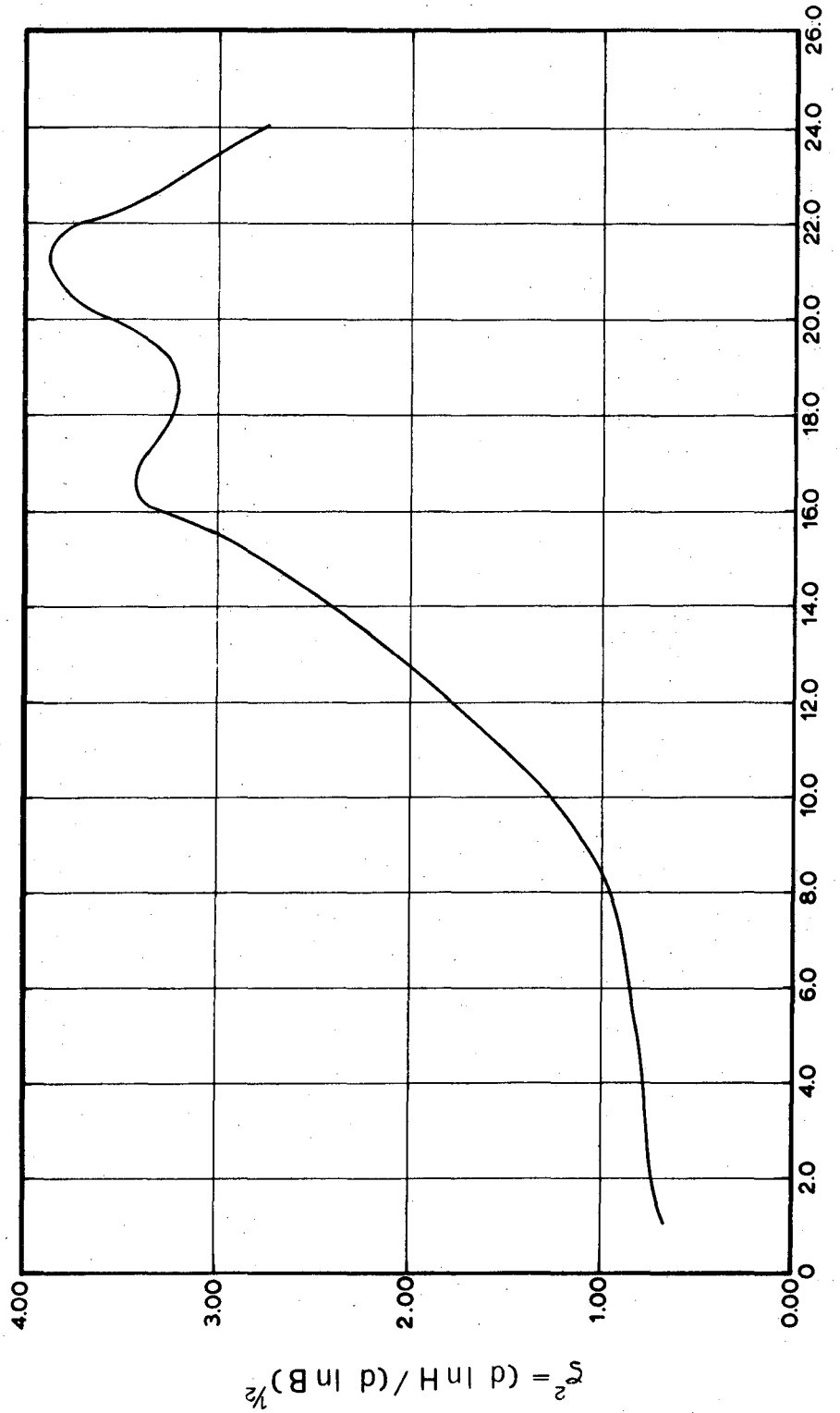
$\zeta^2 = (d \ln H / d \ln B)^{1/2}$
4.00
3.00
2.00
1.00
0.00
0
2.0
4.0
6.0
8.0
10.0
12.0
14.0
16.0
18.0
20.0
22.0
24.0
26.0
B - kilogauss
XBL 7012 6269

Fig. 3B

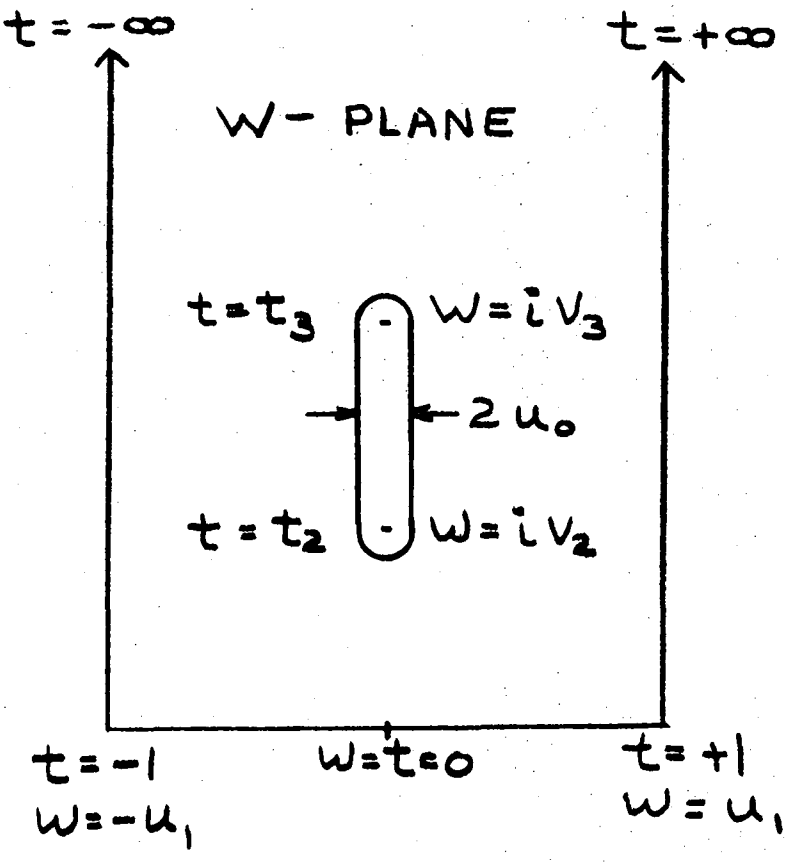


FIG. 4

XBL 7210-1993

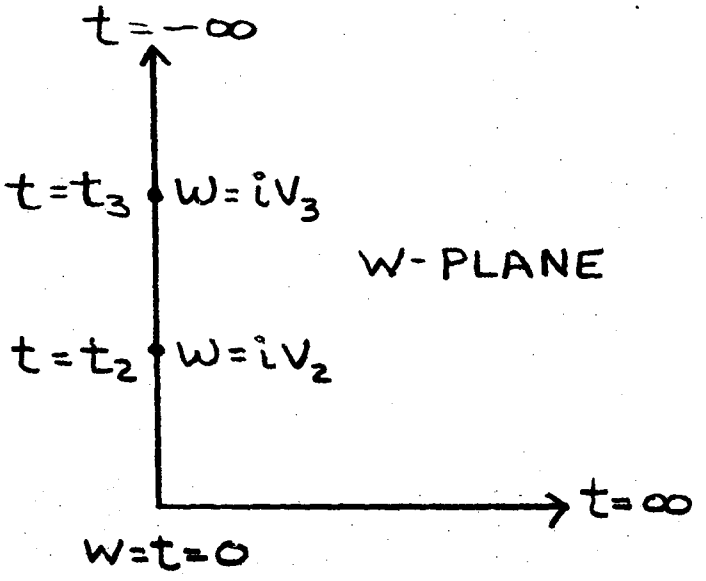


FIG. 5 A

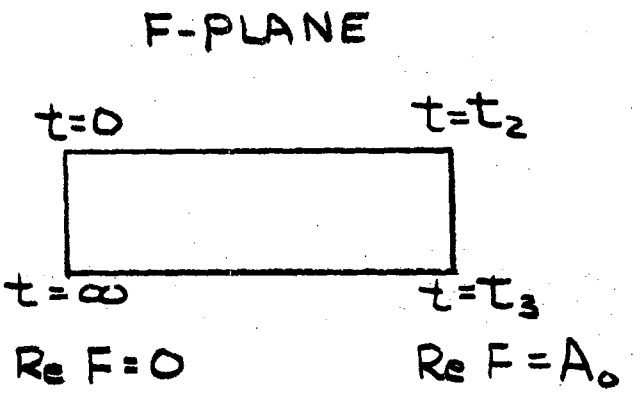


FIG. 5 B

XBL 7210-1992



UCRL-18969

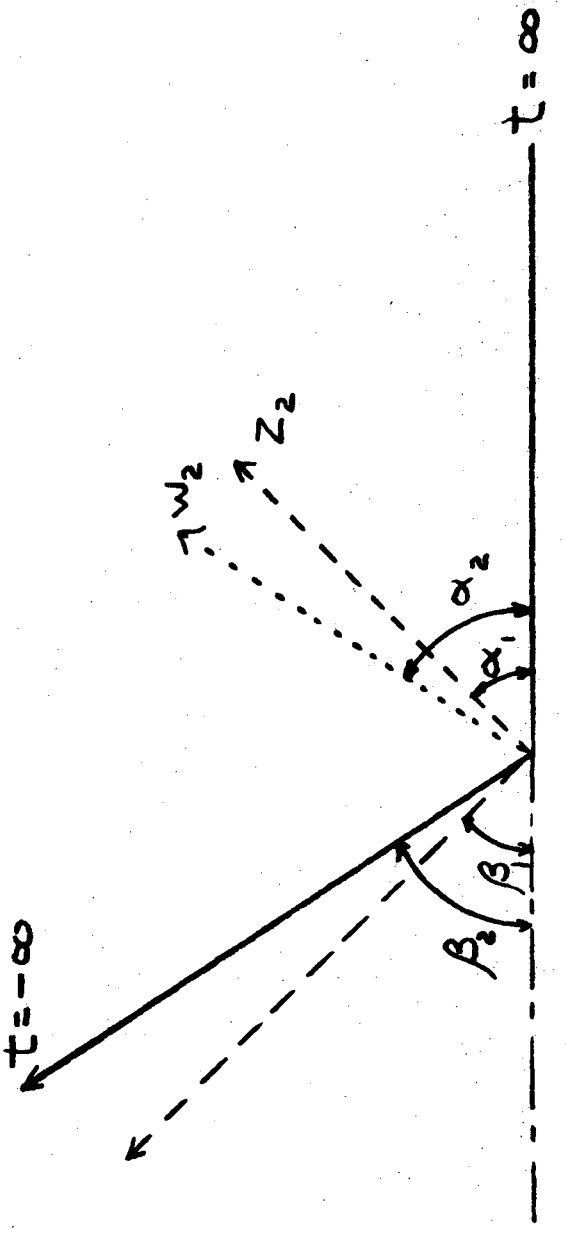


XBL 7210-1972

FIG. 6

*TECHNICAL INFORMATION DIVISION*
*LAWRENCE BERKELEY LABORATORY*
*UNIVERSITY OF CALIFORNIA*
*BERKELEY, CALIFORNIA 94720*